Cell Reports, Volume *43*

Supplemental information

ATM-deficiency-induced microglial activation promotes neurodegeneration in ataxia-telangiectasia

Jenny Lai, Didem Demirbas, Junho Kim, Ailsa M. Jeffries, Allie Tolles, Junseok Park, Thomas W. Chittenden, Patrick G. Buckley, Timothy W. Yu, Michael A. Lodato, and Eunjung Alice Lee

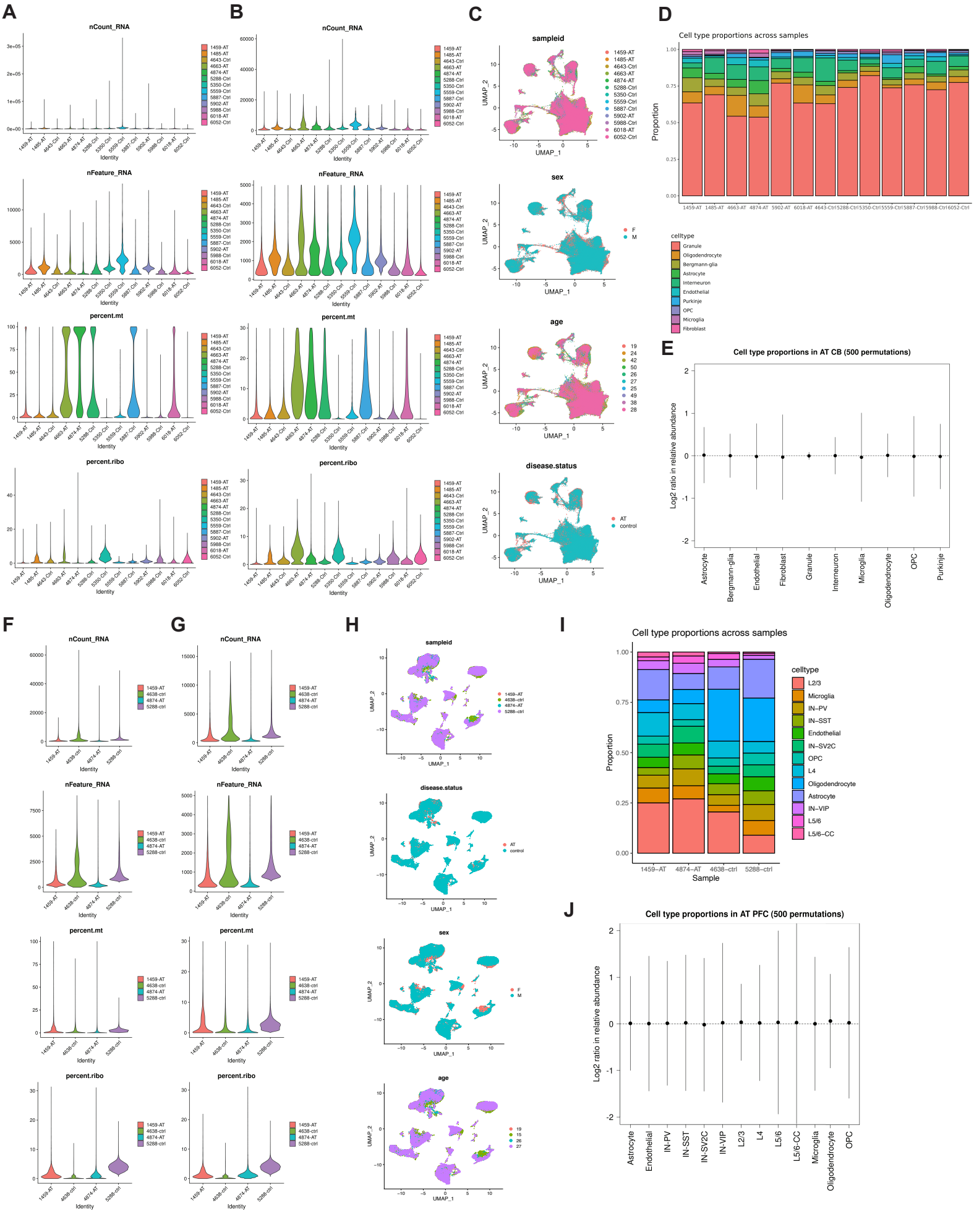
A
B
C
D
nCount_RNA
nFeature_RNA
percent.mt
percent.ribo
sampleid
sex
age
disease.status
UMAP_1
UMAP_2
Identity
Cell type proportions across samples
Proportion
celltype
Granule
Oligodendrocyte
Bergmann-glia
Astrocyte
Interneuron
Endothelial
Purkinje
OPC
Microglia
Fibroblast
E
Cell type proportions in AT CB (500 permutations)
Log2 ratio in relative abundance
Astrocyte
Bergmann-glia
Endothelial
Fibroblast
Granule
Interneuron
Microglia
Oligodendrocyte
OPC
Purkinje
F
G
H
I
Cell type proportions across samples
Sample
L2/3
Microglia
IN–PV
IN–SST
Endothelial
IN–SV2C
OPC
L4
Oligodendrocyte
Astrocyte
IN–VIP
L5/6
L5/6–CC
J
Cell type proportions in AT PFC (500 permutations)
Astrocyte
Endothelial
IN-PV
IN-SST
IN-SV2C
IN-VIP
L2/3
L4
L5/6
L5/6-CC
Microglia
Oligodendrocyte
OPC

Fig. S1. Quality control information for snRNA-seq data from cerebellum and PFC, Related to Figure 1 and Figure 2. A. Transcript (nCount_RNA), gene (nFeature_RNA), percent transcripts from mitochondrial genes, and percent transcripts from ribosomal genes per cerebellar sample before quality control filtering. B. Transcript (nCount_RNA), gene (nFeature_RNA), percent transcripts from mitochondrial genes, and percent transcripts from ribosomal genes per cerebellar sample after quality control filtering. C. UMAP plots of cerebellar data showing integration of samples, sex, age, and disease status. D. Stacked barplots showing proportion of each cell type per cerebellar sample. E. Posterior distribution of log2 ratio of cell type proportions in A-T cerebellum after 500 random permutations. F. Transcript (nCount_RNA), gene (nFeature_RNA), percent transcripts from mitochondrial genes, and percent transcripts from ribosomal genes per PFC sample before quality control filtering. G. Transcript (nCount_RNA), gene (nFeature_RNA), percent transcripts from mitochondrial genes, and percent transcripts from ribosomal genes per PFC sample after quality control filtering. H. UMAP plots of cerebellar data showing integration of samples, disease status, sex, and age. I. Stacked barplots showing proportion of each cell type per PFC sample. J. Posterior distribution of log2 ratio of cell type proportions in A-T PFC after 500 random permutations.

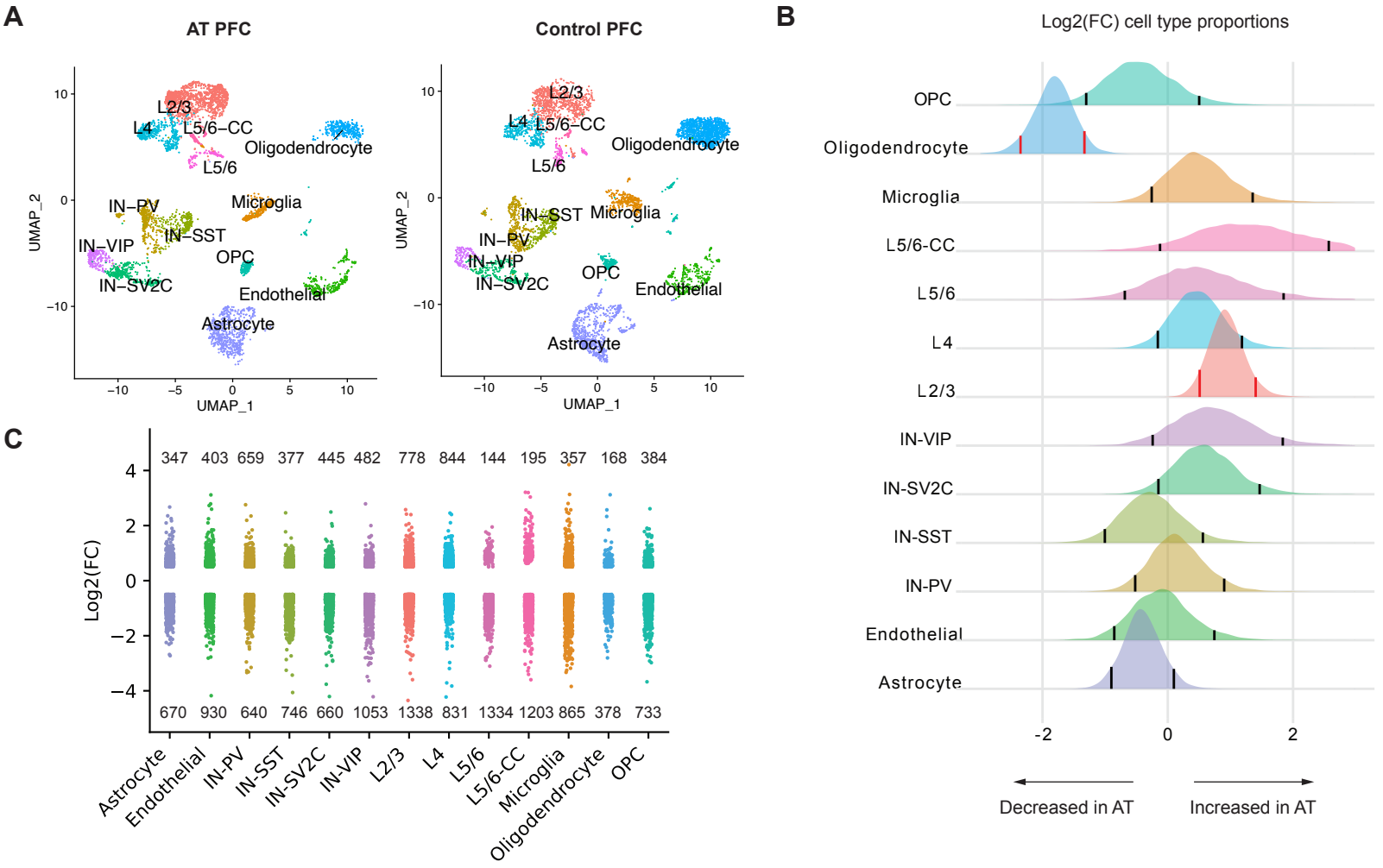

Fig. S2. snRNA-seq data of A-T PFC, Related to Figure 1. A. UMAP plot of major cell types in AT and control human PFC, downsampled to 10,000 cells per condition only for visualization purpose. B. Relative abundance of cell types in AT versus control PFC, shown as the posterior distribution of Log2(proportion in AT/proportion in control) with 89% credible interval. Red bars highlight credible intervals that do not overlap 0. Bolded cell type labels indicate a significant difference in relative abundance. C. Differentially expressed genes (DEGs) in each cell type with FDR<0.05, |Log2FoldChange|>0.50. Each dot represents a significantly differentially expressed gene.

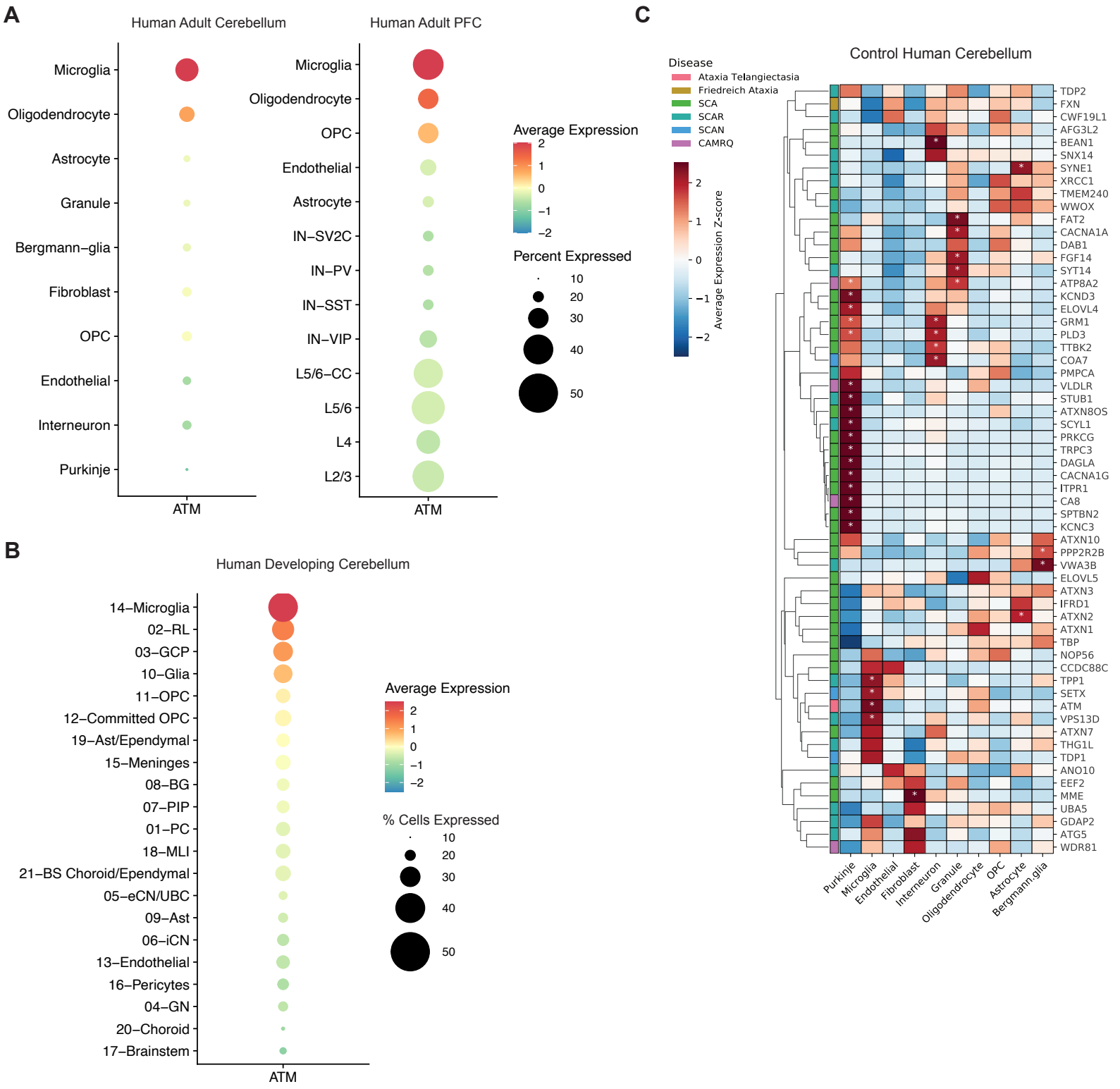

Fig. S3. Enriched expression of monogenic cerebellar disease genes in specific cell types, Related to Figure 2. A. Dotplot of average scaled expression of ATM in cell types of the adult human cerebellum and prefrontal cortex, and B. developing human cerebellum (Aldinger et al., 2021). Microglia have the highest expression of ATM out of all cell types in the cerebellum and PFC. Size of dot represents percentage of single cells expressing the gene. Expression scaled to mean of 0 and standard deviation of 1. C. Heatmap of cerebellar ataxia disease gene expression across cell types in control human cerebellum. Color represents centered and scaled log-normalized expression. *Enrichment p-value <0.05. OPC: oligodendrocyte precursor cell, IN-SV2C: SV2C expressing inhibitory neuron; IN-PV: PVALB expressing inhibitory neuron; IN-SST: SST expressing inhibitory neuron; L5/6-CC: layer 5/6 cortico-cortical neuron; L5/6: layer 5/6 neuron; L4: layer 4 neuron; L2/3: layer 2/3 neuron; 01-PC: Purkinje cells; 02-RL: Rhombic lip; 03-GCP: Granule cell progenitors; 04-GN: Granule neurons; 05-eCN/UBC: Excitatory cerebellar nuclei neurons/ Unipolar brush cells; 06-iCN: Inhibitory cerebellar nuclei neurons; 07-PIP: PAX2+ interneuron progenitors; 08-BG: Bergmann glia; 09-Ast: Astrocytes; 10-Glia: Glia; 11-OPC: Oligodendrocyte precursor cells; 12-Committed OPC: Committed oligodendrocyte precursor cells; 13-Endothelial: Endothelial cells; 14-Microglia: Microglia; 15-Meninges: Meninges; 16-Pericytes: Pericytes; 17-Brainstem: Brainstem; 18-MLI: Molecular layer interneurons; 19-Ast/Ependymal: Astrocytes/ependymal cells; 20-Choroid: Choroid plexus; 21-BS Choroid/Ependymal: Choroid plexus/ependymal cell; SCA: spinocerebellar ataxia; SCAR: spinocerebellar ataxia, recessive; SCAN: spinocerebellar ataxia, autosomal recessive, with axonal neuropathy; CAMRQ: cerebellar ataxia, impaired intellectual development, and dysequilibrium syndrome.

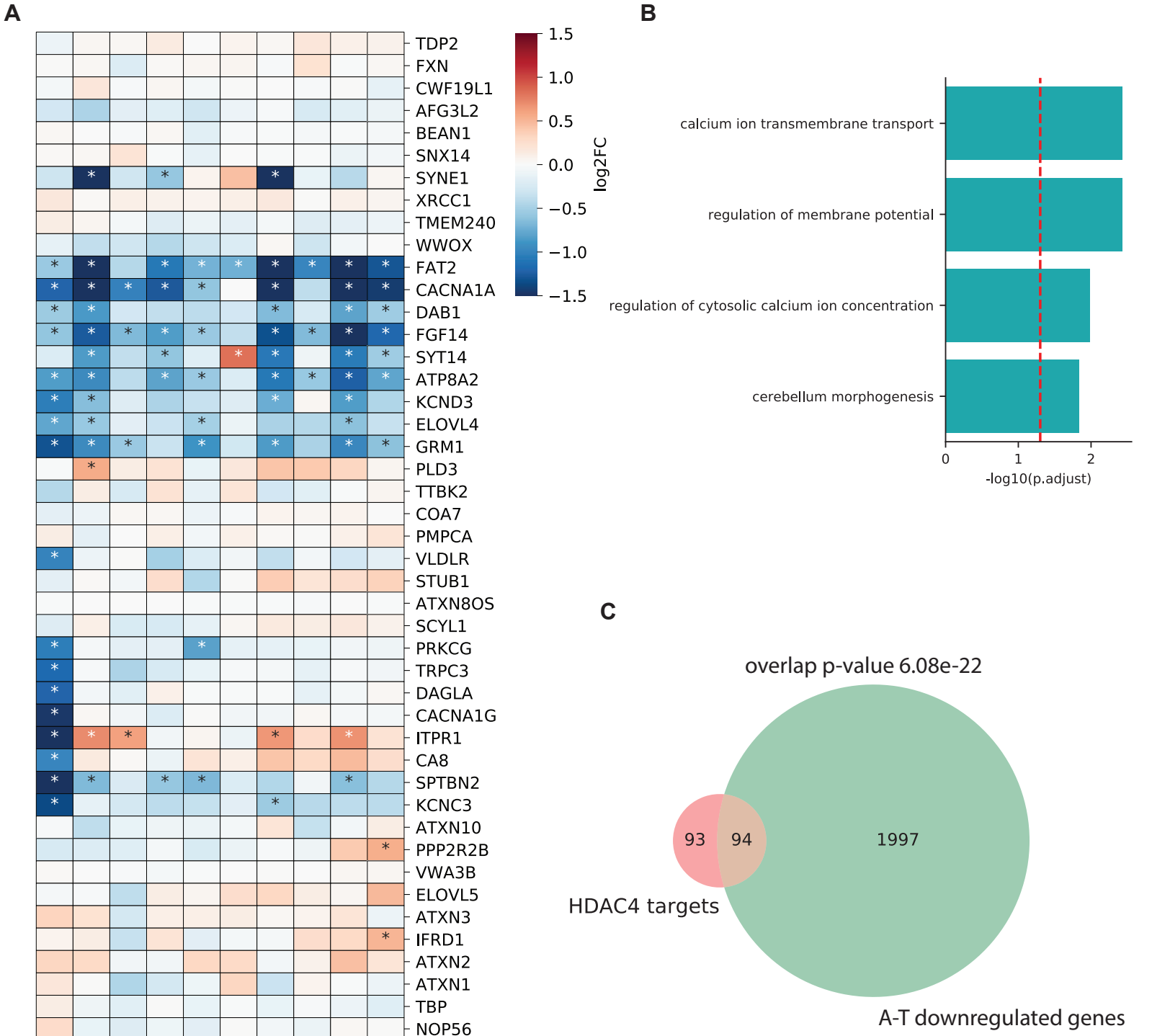

Fig. S4. Dysregulation of hereditary ataxia genes in A-T, Related to Figure 3. A. Heatmap showing log2 fold-change of hereditary ataxia genes in A-T cerebellum. *FDR<0.05. ATM expression increased in several cell types in A-T cerebellum, suggesting that lack of ATM function induces compensatory increases in transcription of the ATM locus. B. Enriched Gene Ontology (GO) pathways among disease genes with enriched expression in Purkinje cells and downregulated in A-T Purkinje cells. C. Overlap between HDAC4 neuronal target genes and downregulated DEGs in A-T cerebellum.

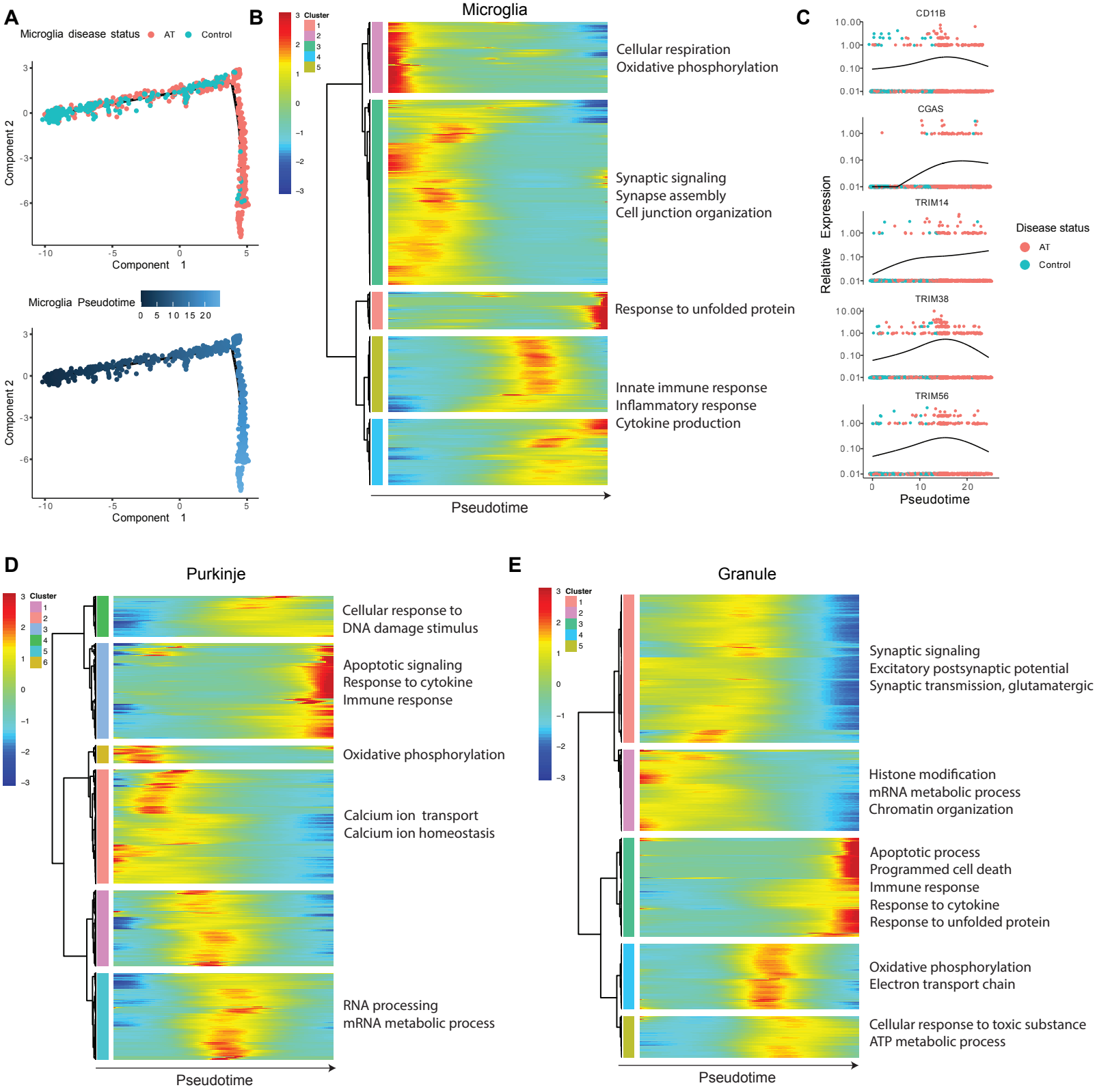

Fig. S5. Pseudotime analysis of disease progression reveals early microglia activation, Related to Figure 6. A. Disease progression pseudotime trajectory of A-T cerebellar microglia, colored by disease status (red: A-T, blue: control), or pseudotime (healthy to diseased). B. Heatmap of genes that significantly change over pseudotime in microglia, clustered by pseudotemporal expression patterns. Each cluster is annotated with enriched GO terms (FDR<0.05). C. Expression of CD11B, CGAS, TRIM14, TRIM38, and TRIM56 over pseudotime in microglia. D. Heatmap of genes that change over pseudotime in Purkinje neurons, clustered by pseudotemporal expression patterns. Each cluster is annotated with enriched GO terms (FDR<0.05). E. Heatmap of genes that change over pseudotime in granule neurons, clustered by pseudotemporal expression patterns. Each cluster is annotated with enriched GO terms (FDR<0.05). Heatmaps in B, D, E depict centered and scaled expression.

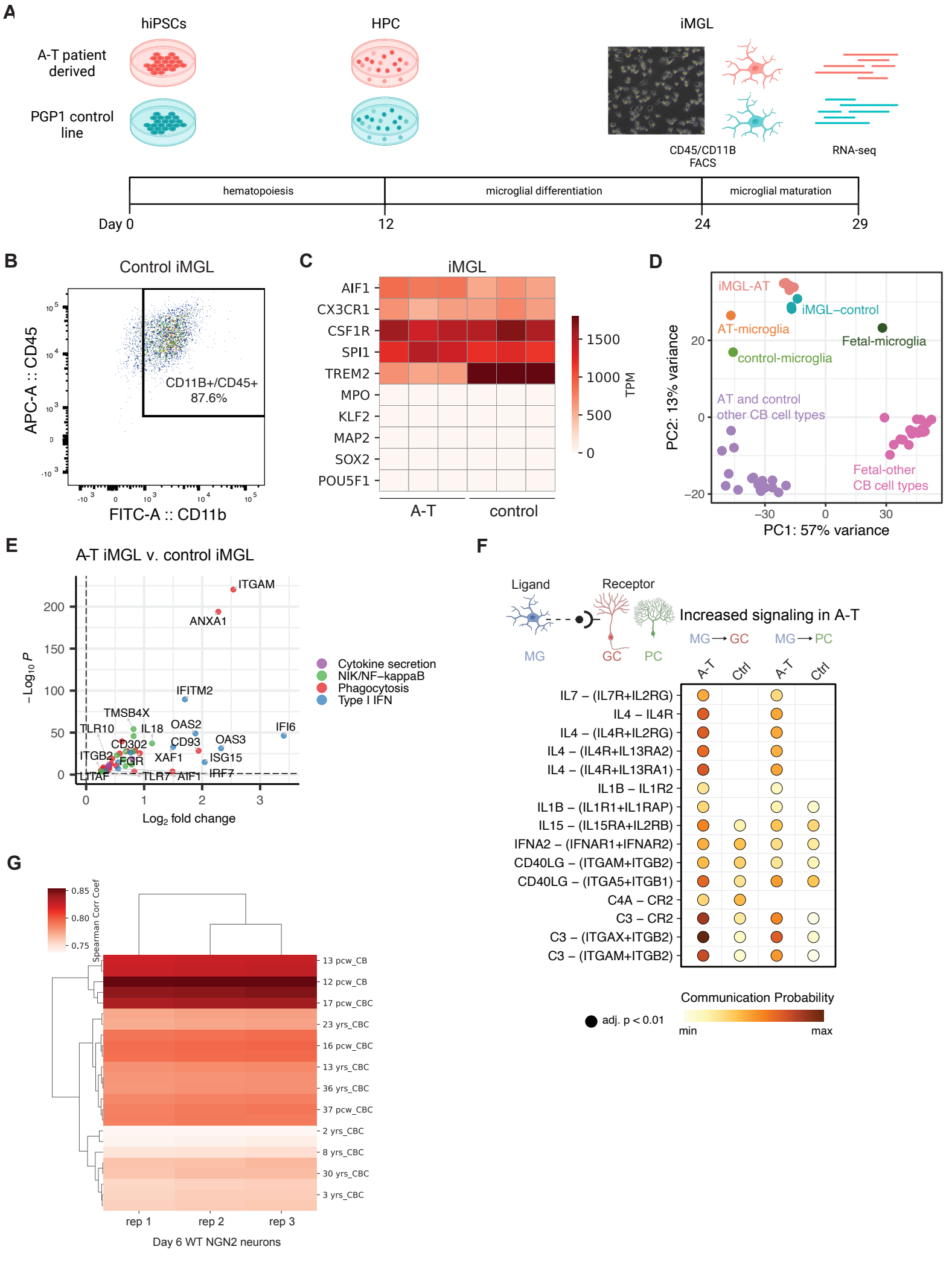
A
hiPSCs
HPC
iMGL
A-T patient derived
PGP1 control line
CD45/CD11B FACS
RNA-seq
hematopoiesis
microglial differentiation
microglial maturation
Day 0
12
24
29
B
Control iMGL
APC-A :: CD45
FITC-A :: CD11b
CD11B+/CD45+ 87.6%
C
iMGL
AIF1
CX3CR1
CSF1R
SPI1
TREM2
MPO
KLF2
MAP2
SOX2
POU5F1
TPM
1500
1000
500
0
A-T
control
D
iMGL-AT
iMGL–control
AT-microglia
Fetal-microglia
control-microglia
AT and control other CB cell types
Fetal-other CB cell types
PC2: 13% variance
PC1: 57% variance
E
A-T iMGL v. control iMGL
ITGAM
ANXA1
IFITM2
TMSB4X
TLR10
IL18
OAS2
IFI6
CD302
CD93
OAS3
ITGB2
FGR
XAF1
ISG15
LITAF
TLR7
AIF1
IRF7
Cytokine secretion
NIK/NF–kappaB
Phagocytosis
Type I IFN
−Log10 P
Log2 fold change
F
Ligand
Receptor
MG
GC
PC
Increased signaling in A-T
MG → GC
MG → PC
A-T
Ctrl
IL7 – (IL7R+IL2RG)
IL4 – IL4R
IL4 – (IL4R+IL2RG)
IL4 – (IL4R+IL13RA2)
IL4 – (IL4R+IL13RA1)
IL1B – IL1R2
IL1B – (IL1R1+IL1RAP)
IL15 – (IL15RA+IL2RB)
IFNA2 – (IFNAR1+IFNAR2)
CD40LG – (ITGAM+ITGB2)
CD40LG – (ITGA5+ITGB1)
C4A – CR2
C3 – CR2
C3 – (ITGAX+ITGB2)
C3 – (ITGAM+ITGB2)
adj. p < 0.01
Communication Probability
min
max
G
Spearman Corr Coef
0.85
0.80
0.75
13 pcw_CB
12 pcw_CB
17 pcw_CBC
23 yrs_CBC
16 pcw_CBC
13 yrs_CBC
36 yrs_CBC
37 pcw_CBC
2 yrs_CBC
8 yrs_CBC
30 yrs_CBC
3 yrs_CBC
rep 1
rep 2
rep 3
Day 6 WT NGN2 neurons

Fig. S6. A-T patient iPSC-derived microglia reveal cell-intrinsic activation of NF-kappaB and type I interferon pathways, Related to Figure 6. A. Schematic for generation of iPSC-derived microglia (iMGL) from human A-T patient and control iPSCs. PGP1, Personal Genome Project 1; HPC: hematopoietic progenitor cells. B. Flow cytometry analysis of CD45 and CD11B co-expression in control iMGLs 24 days post-differentiation. C. Expression of microglia (AIF1, CX3CR1, CSF1R, SPI1, TREM2), myeloid lineage (MPO, KLF2), neuronal (MAP2, SOX2), and iPSC (POU5F1) marker genes in A-T and control iMGLs. Each column represents data from iMGL differentiated in an independent well. D. Principal component analysis plot of A-T and control iMGL (iMGL-AT/control) and adult cerebellar cell type pseudobulk transcriptomic profiles derived from snRNA-seq in this study (AT/control-microglia) and fetal cerebellar cell type pseudobulk transcriptomic profiles derived from snRNA-seq data in Aldinger et al., 2021 (Fetal-microglia). E. Volcano plot for log2 fold change in gene expression in A-T versus control iMGL. Representative genes associated with cytokine secretion (purple), NIK/NF-kappaB (green), phagocytosis (red), and type I interferon (IFN) (blue) are highlighted. Horizontal dash line represents FDR=0.05. F. Ligand-receptor pairs with increased communication probability from microglia to granule or Purkinje neurons in A-T cerebellum versus control. Dot color represents communication probability (strength of signaling). Dot size represents significance of ligand-receptor pair and pairs with adjusted p-value<0.01 shown. G. Heatmap of Spearman Correlation Coefficients between human control PGP1 (WT) iPSC-derived Ngn2 neurons at day 6 of differentiation transcriptomes and human developing cerebellum (CB) and cerebellar cortex (CBC) transcriptomes from BrainSpan: Atlas of the Developing Human Brain.